

Comparative Analysis of the Friction and Microstructural Properties of WC-10Co-4Cr and Cr₃C₂-25NiCr Coatings Sprayed by High-Velocity Oxy-fuel (HVOF)

Angela Selau Marques^{*}, Rafael Luciano Dalcin, Leonardo Fonseca Oliveira,
Lucas Alves Vitor da Silva, Giovanni Rocha dos Santos, Alexandre da Silva Rocha

Department of Metallurgical Engineering, UFRGS - Federal University of Rio Grande do Sul, Porto Alegre-RS, Brazil

Abstract In this study, coatings WC-10Co-4Cr and Cr₃C₂-25NiCr were deposited on the AISI H13 steel by oxy-fuel Thermal spraying (HVOF). This coating increases the wear resistance of surfaces subjected to severe conditions, such as: abrasive wear, thermal fatigue and plastic deformation. The coatings microstructure, hardness and wear resistance are investigated through friction and wear tests performed through a pin-on-disc type tribometer following the procedures defined in ASTM G99-04. It was verified that both materials used in the spraying have high resistance to wear, however, in the sample coated with Cr₃C₂-25NiCr there was a greater removal of material during the test.

Keywords Wear, Friction, Thermal Spraying

1. Introduction

Chromium and Tungsten Carbide coatings are used to improve wear resistance in industry various segments and recently it has also been applied in the mechanical forming industry to prevent premature damage to the die caused by the hot forging process [1]. Coatings based on cermets can be applied by High-Velocity Oxy-fuel Spraying (HVOF), which is a promising technique and has stood out from the rest due to its characteristics [2]. Table 1 presents a comparison between the main characteristics of PVD coatings used by the metalworking industry. The choice of coating to be used depends greatly on the application, however the versatility of coatings applied by thermal spraying has made its use increase considerably in recent years [3].

Researches developed by Murthy et al. (2001) show that carbide-containing coatings deposited by HVOF have good wear resistance compared to plasma spray coatings, this is due to the better coating properties that can be obtained by the processes of high speed [5]. HVOF is a suitable technique for sprinkling of materials such as WC, due to high impact velocities and low sprinkling temperature. The WC particles give the coating high level of hardness and wear resistance,

while the Co, Ni, and Cr materials provide toughness [6]. The main phenomena that occur during thermal spraying processes, which influence coating performance, are the oxidation and the high temperature decomposition of tungsten carbide [7]. Experiments carried out by Mateen et al. (2011) revealed that WC-Co coatings have high wear resistance, good mechanical properties and, in addition, good control of the tribological properties can be obtained [8].

Table 1. Comparison between coatings

Characteristics	PVD	Thermal Sprinkler
Operating cost	Moderate to high	Low to high
Process environment	Hard Vacuum	Atmospheric to soft Vacuum
Coating thickness	Very thin to moderate	Thick
Substrate Temperature	Low	Low to Moderate
Adherence	Moderate mechanical bond to good chemical bond	Good mechanical bond
Surface finish	Smooth to high gloss	Coarse to smooth

The wear behavior of the WC-based coatings with Co deposited by different thermal spraying processes were studied by several researchers [5, 6, 9, 10]. The studies developed by the aforementioned authors report that the hardness, fracture strength and adhesion strength between the hardened layer and the die are the most important factors

* Corresponding author:

angela_selau@ufrgs.br (Angela Selau Marques)

Published online at <http://journal.sapub.org/materials>

Copyright © 2018 The Author(s). Published by Scientific & Academic Publishing

This work is licensed under the Creative Commons Attribution International

License (CC BY). <http://creativecommons.org/licenses/by/4.0/>

in the resistance to wear and failure of coatings made from cermet. Murthy *et al.* (2001) applied WC-10Co-4Cr and Cr3C2-20 (NiCr) on a mild steel through the HVOF thermal spraying process. According to the results presented in this research the WC-based coating has a better resistance to abrasive wear compared to the CrC-based coating. In addition, the carbide based coatings applied via HVOF have excellent wear resistance compared to other application methods.

2. Experimental Procedures

In the present study, WC-10Co-4Cr and Cr3C2-25NiCr coatings were deposited via HVOF. The coatings were characterized by X-ray diffraction, optical microscopy, scanning electron microscopy (SEM) and microhardness. Finally, both coatings wear resistance is compared through a pin-on-disc type tribometer, following the procedures defined in ASTM G99-04. This test provides friction and wear resistance information under dry sliding conditions.

The specimens used in the test were fabricated from AISI H13 steel by the conventional machining process. The dimensions are 60 mm in diameter and 15 mm in thickness. After the parts were manufactured, the tempering and tempering treatment was carried out according to the material specifications, reaching a hardness of 51 HRC.

2.1. Coating Materials

The method of manufacturing the material determines the powders morphology and may vary according to the supplier. This characteristic has a great influence on the heat exchange between the particles and the combustion gases, since the size and shape of the powder influence the ability to absorb thermal energy during the deposition process [11, 12]. The powders morphology also determines the lamellar structure, by the way the particles settle when they collide with the substrate [13]. In this study, two types of powders were used, supplied by Oerlikon Metco. The main characteristics of each one are represented in Table 2.

Table 2. Characteristics and properties of the materials used in the spraying

Main information		
Classification	Carbides based on Chromium	Carbides based on Tungsten
Chemical composition	Cr3C2-25NiCr	WC10Co4Cr
Manufacturing	Synthetic and sintered	Sintered and compressed
Morphology	Spheroidal	Angular / blocks
Apparent density	2.3 to 3.1 g/cm ³	4,8 to 5,0 g/cm ³
Operating temperature	<870°C	≤ 500°C

2.2. Spraying HVOF

The coatings were applied on H13 samples. Prior to the coating application, the samples undergo a blasting process with aluminum oxide. This procedure has the purpose of

increasing the surface roughness to improve the adhesion of the coating to the substrate [15]. The coating deposition was performed by the company Rijeza Metallurgy. This company is specialized in the development and application of wear coatings on machines, equipment and parts in different segments of the metalworking industry. For application of the coating the TAFE JP 5000 HP / HVOF System Model 5120, from the manufacturer PRAXAIR and a TAFE GUN Model 5220 pistol, was used as shown in Fig. 1.

A summary of the process main characteristics are presented in Table 3. These configurations define characteristics of the coating, such as: layer thickness, lamellar structure, porosity, etc. The expected thickness of the coating is 200 μm. After application of the coating the parts are cooled in the air.



Figure 1. Application of the coating on the specimens

Table 3. Thermal Sprinkler Process Parameters

Description	Values
Feed rate	80-90 g/min
Nitrogen pressure	70 PSI
Fuel pressure	120±10 PSI
Distance from gun to test piece	300 mm
Gun displacement speed	850 mm/min

2.3. Characterization Tests

After application of coating via HVOF, the samples were cut and sanitized for the assays. Scanning electron microscopy (SEM) analysis was performed in Zeiss Scanning Electron Microscope EVO MA 10, which allows analyzing the grain morphology used in the spray and the surface after the coatings were applied. X-ray diffraction analyzes were performed using a Charon XRD Mcom X-ray diffractometer with Cr-K rad radiation. The model GE Meteor1D detector, of the linear type of 20° was used. In addition, the sample was rotated around the PHI axis at an angular velocity of 0.5 / s with an amplitude of 45° and displaced in oscillatory movements with respect to the X and Y axes at a speed of 0.5 mm / s and amplitude of 5 mm. Measurements were taken for 2 angles ranging from 35° to 166° with a pitch of 0.02° and a measurement time per step of 200 seconds. Vickers microhardness measurements were performed in accordance with the international standard ASTM E92 [17]. The Vickers HV0.01 microhardness

profiles were constructed using an ISH-TDV 1000 microdurometer model - Micro Hardness Tester - INSIZE. The charge penetration time was 10 seconds. Measurements were taken in the cross section of the sample.

2.4. Pin-on-disc Test and Wear Track Measurement

The standard governing the pin-on-disc test is designated by ASTM as G99-04 [18]. This regulation provides a standard, laboratory-level method for conducting material wear tests during sliding using the pin-on-disc configuration. A ceramic ball (Al_2O_3) of 6 mm with an average hardness of 1528 HV was used, applying a normal force (F) of 30N. During the test, the linear velocity produced was 0.47 m/s in a radius of 18 mm, with a total distance of 1000 m. For each coating three replications were performed. The measurements of width, depth of wear tracks, and consequently the coatings volume loss produced by this test were obtained by means of profilometry. The roughness of the coated surface was characterized by a BRUKER 3D Optical Profilemeter and the Vision64® analysis software from the Multi-user Surface Analysis Laboratory (LAMAS) at UFRGS.

3. Results and Discussion

3.1. X-ray Diffraction Analysis

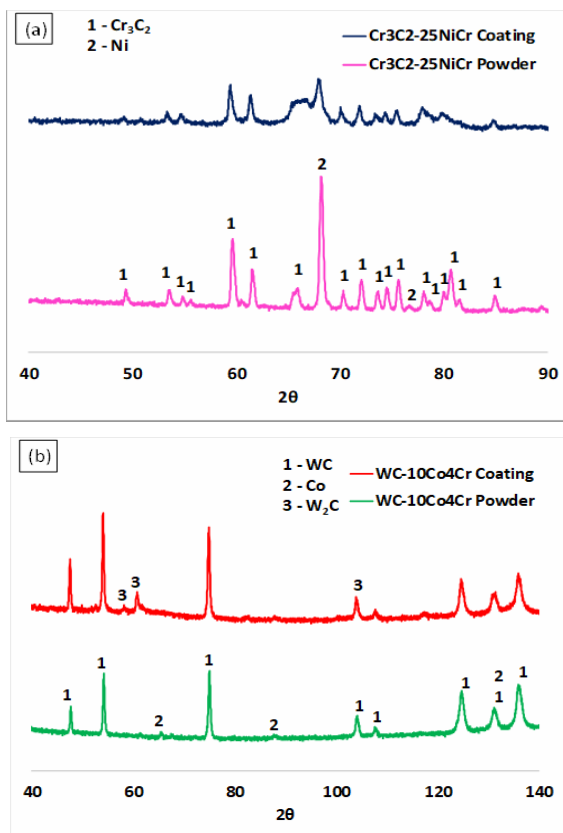


Figure 2. XRD patterns of coatings and powder. (a) Cr₃C₂-25NiCr and (b) WC-10Co₄Cr

Fig. 2 (a) shows the diffractogram for Cr₃C₂-25NiCr

powder and the coated surface. In the standard obtained for the powder several peaks of the Cr₃C₂ phase and an intense Ni peak are present. After the powder is sprayed the Ni peak becomes less intense and closer to one of the peaks of Cr₃C₂, becoming wider, characterizing an amorphous phase. Similar results were also obtained by Murthy & Venkataraman [19]. Other peaks defined in the powder were less evident after the sprinkling process. The increase in the formation of non-crystalline amorphous phases occurs due to very fast cooling during the spraying process [20].

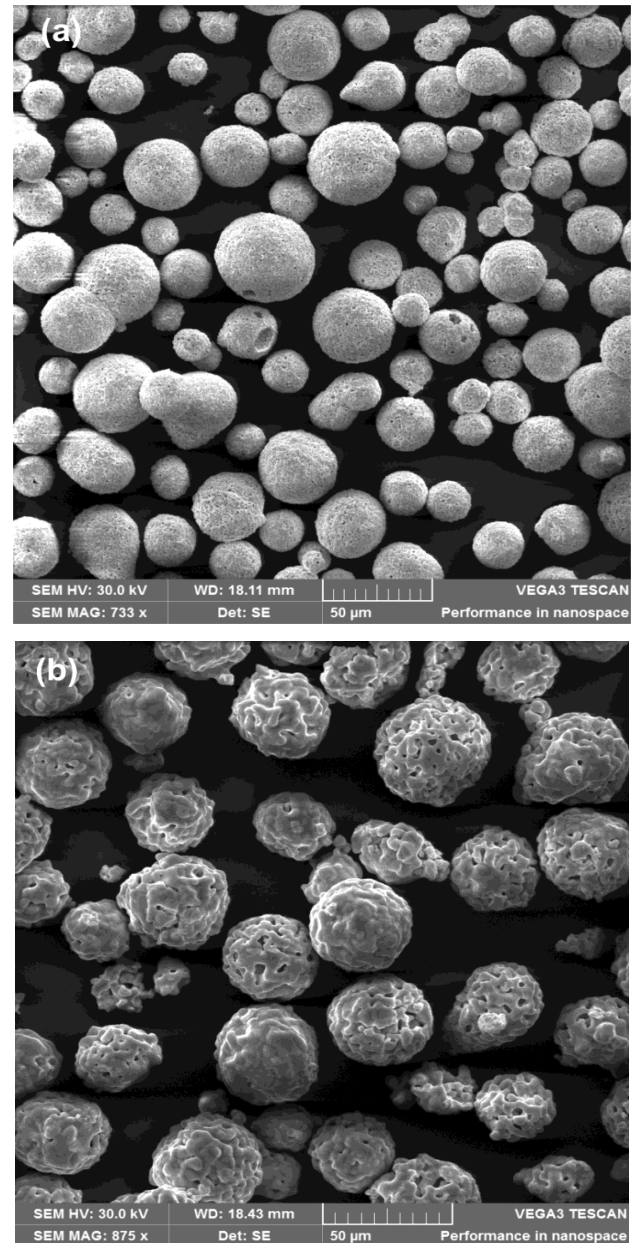


Figure 3. Morphology of the powder used in the coating based. (a) Cr₃C₂-25NiCr and (b) WC-10Co₄Cr

The results obtained for the WC-10Co₄Cr powder and for the coated surface are presented in the difatogram of Fig. 2 (b). The presence of the WC and Co. phases can be observed. After the coating deposition, characteristic peaks and "elbows" of the W₂C phase are formed. This dewaxing of

WC in W2C may impair some coating properties due to the formation of brittle carbides [15, 19]. Studies developed by Stewart, Shipway & McCartney demonstrate that the amount of different phases and the proportion of each depends greatly on the process conditions at the time of spraying the particles under the substrate. [21].

3.2. Microstructural Characterization

Fig. 3 (a) shows the scanning electron microscopy (SEM) analysis of the morphological characteristics of WC-10Co4Cr powder. This material has a dense grain, which forms a more homogeneous layer, because material spreads better on the surface [22]. This morphology is desirable for the Thermal spraying y process by HVOF, as it allows a better flow of the powder in the spray gun during the application of the coating [23]. The average diameter of the beads of WC-10Co4Cr powder is 30 μm . In Fig. 3 (b) it is observed that the morphology of Cr3C2-25NiCr powder presents a hollow sphere shaped structure with porosities and spaced particles, the grain diameter varies around 40 μm .

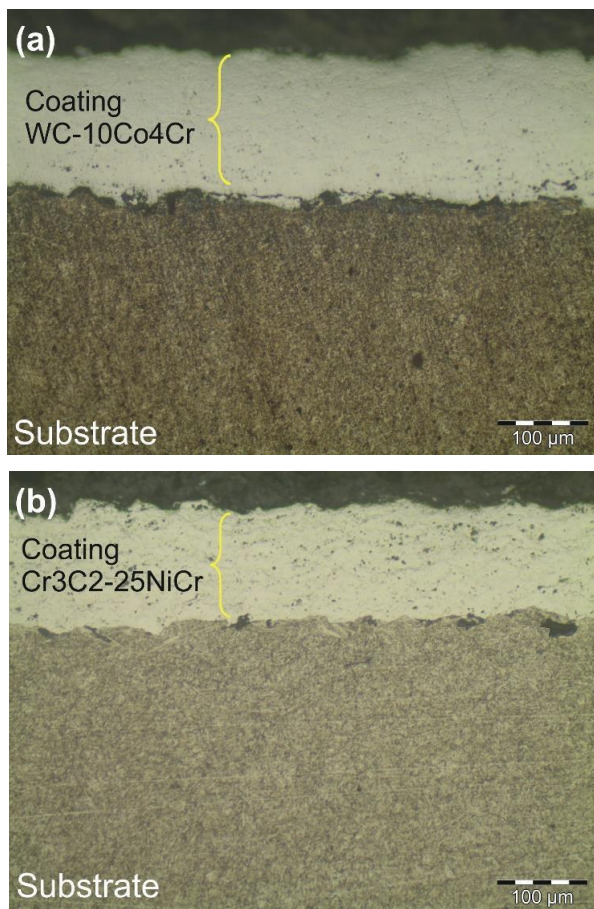


Figure 4. Microestrutura dos revestimentos. (a) WC-10Co4Cr. (b) Cr3C2-25NiCr

In Fig. 4 (a) and (b) the cross-sectional optical micro-graphs are shown for both coatings. Fig. 4 (a) shows the WC-10Co4Cr coated specimen, the mean thickness of this layer is 122 μm and the average roughness was about 3

μm after coating application. Fig. 4 (b) shows the specimen coated with Cr3C2-25NiCr, the layer has a mean thickness of 118 μm and a mean roughness of 2 μm .

It is possible to visualize in Fig. 5 (a) and (b) that both coatings have pores, voids and a layer with lamellar structure, containing in their outline a discrete oxide film, a common feature of coatings applied via HVOF. This occurs due to the overlapping of high-speed melt and semi-fused particles deposited on the substrate [24]. The ImageJ program was used to measure porosity. The Cr3C2-25NiCr coating had a higher pore concentration, around 1.2% and the WC-10Co4Cr coating had 0.9% of its pore area. Thus, both layers are well constituted and within acceptable limits for this type of coating, as described in the literature [15].

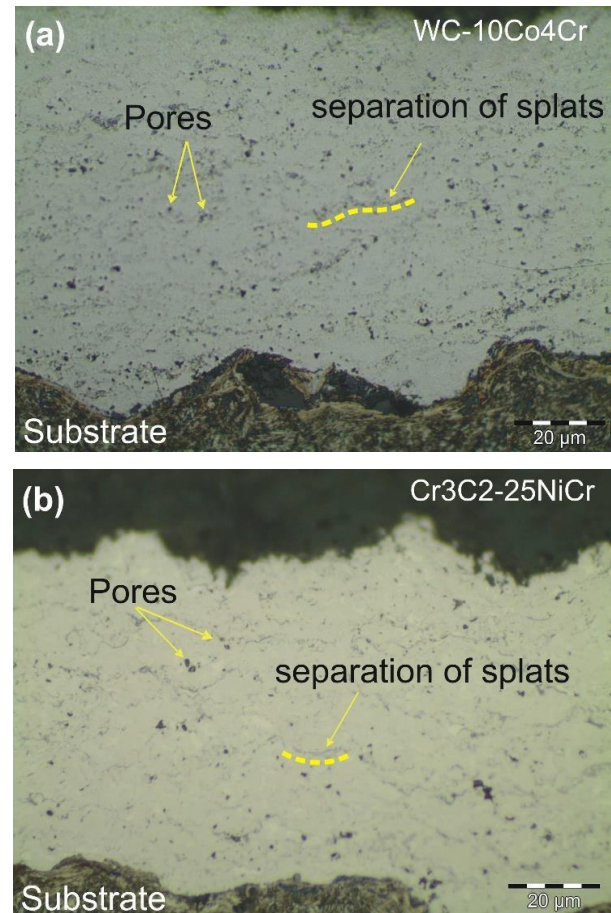


Figure 5. Pores and voids in coatings. (a) WC-10Co4Cr. (b) Cr3C2-25NiCr

The coefficient of adhesion is defined by the force required to remove the coating from the substrate, this parameter is extremely relevant, especially for applications where the coating will be subjected to severe stress. According to the literature and the material manufacturer, the value must be greater than 69 MPa for coatings deposited by Thermal spraying [25, 26]. The test result, following the ASTM C633 standard [27], was 85.6 MPa for the WC-10Co4Cr coated sample, and 71.2 MPa for the sample coated with Cr3C2-25NiCr.

3.3. Microhardness

The average Vickers microhardness results and the standard deviation of each coating are shown in the graph of Fig. 6 (a). The microhardness values of the layer sprayed with Cr₃C₂-25NiCr are lower than WC-10Co₄Cr values. This behavior is compatible with both researched literature and material supplier indications [28]. It will be appreciated that both coatings have high hardness variations along the cross section, this is due to non-uniformity of the layer. Fig. 6 (a) and (b) shows that each indentation point is located in different microstructures, such as carbides, oxides, inclusions and finally the substrate. The substrate measurements do not have values as discrepant as those found in the sprayed layer, which confirms the variation due to the coating characteristics.

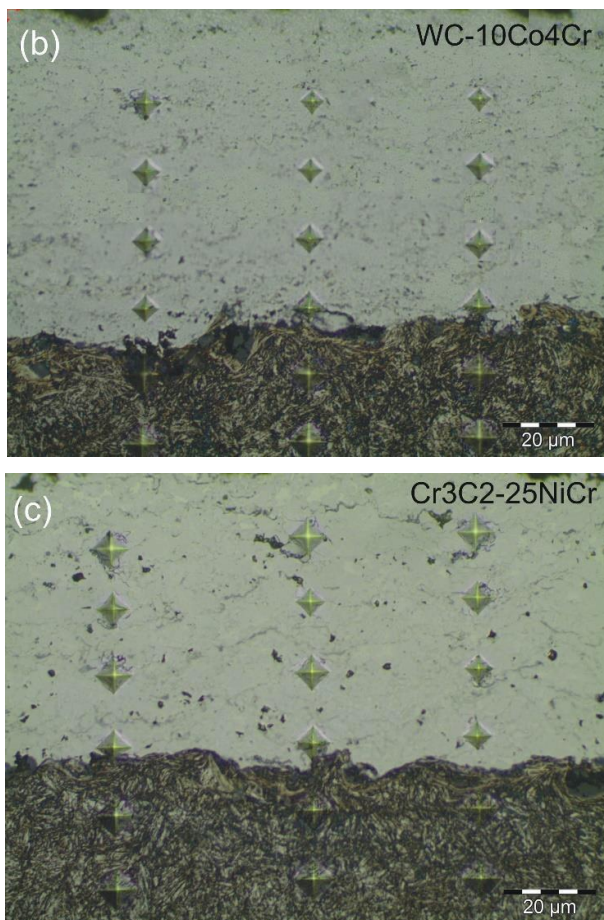
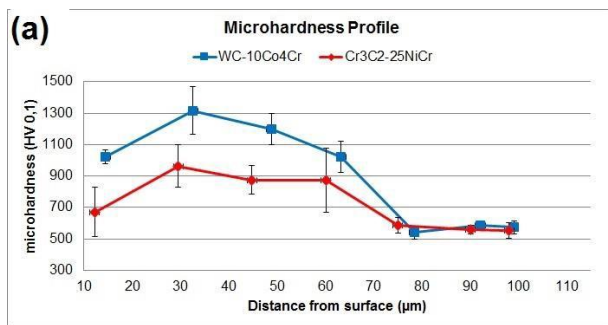


Figure 6. Microhardness profiles of the coatings

3.4. Tribological Behavior - Pin-on-Disc

The behavior of the coefficient of friction for both coatings is shown in Fig. 7. It is observed that the friction coefficient of the sample coated with WC-10Co₄Cr is greater than the sample coated with Cr₃C₂-25NiCr. Initially there is a zone of instability, which occurs due to the detachment of particles from the sphere and the coating [15]. Then, the coefficient of friction reaches a steady value, but there is a maximum and minimum fluctuation that remains constant for both coatings, this phenomenon indicates the wear stabilization on the coating [29, 30].

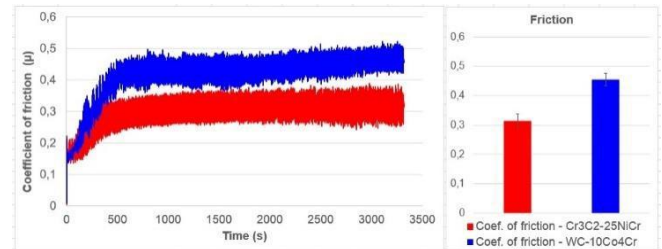


Figure 7. Average coefficient of friction obtained in the pin-on-disc test

In the sample coated with WC-10Co₄Cr the friction is around 0.4. The high hardness and high plasticity of this material favors the adhesion phenomenon during the sliding, raising the coefficient of friction, but difficult the removal of the layer [31, 32].

The sample coated with Cr₃C₂-25NiCr has a coefficient of friction around 0.2. For Vashishtha & Sapate [29], the justification for a low coefficient of friction is the formation of oxides, which generates a thin film of low shear strength, resulting in a decrease in the coefficient of friction. In this path, abrasive wear and plastic deformation occurred, as there was removal of the layer generating a cavity on the surface of the sample.

The pin-on-disc test resulting trails were analyzed by scanning electron microscopy (SEM). In the sample coated with Cr₃C₂-25NiCr, a discrete trail is shown in Fig. 8 (a). In the enlarged image, Fig. 8 (b), there are pores and regions worn by the sliding of the sphere. The results of the WC-10Co₄Cr coated sample are shown in Fig. 8 (c) and (d), it is possible to observe that the track is also discrete and that the sanding marks remain after the test, demonstrating the low volume of material removed. Also notable in Fig. 8 (d) is a mark in the direction of sliding of the ball, effected by a debris particles. These debris particles remain in the tribological systems, between the surfaces in sliding contact, characterizing the abrasion mechanism [33]. With the continuity of this event, the tendency is for the particles to fragment and the abrasive wear rate to decrease [12].

The wear rate of the sample coated with Cr₃C₂-25NiCr was $2.6 \times 10^{-3} \text{ mm}^3$. And the WC-10Co₄Cr sample does not form a track with apparent depth, making it impossible to measure the lost volume. Fig. 9 shows the wear profile of both samples, through this image it is evident that there is no formation of a track with depth in the sample coated with WC-10Co₄Cr.

It is possible to observe that both tracks have a scattered appearance and that even after sanding the roughness remains high, it happens because during the finishing process the most pronounced peaks are eliminated, but the pores remain. In general, coatings applied by HVOF have a low wear rate [29].

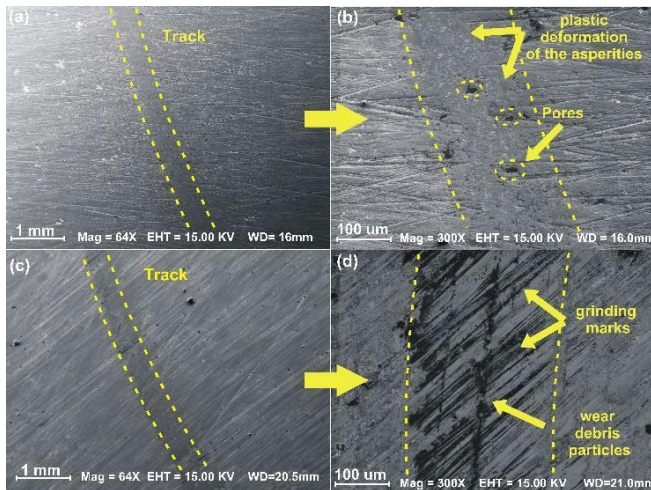


Figure 8. Profilometry of worn tracks after pin-on-disc tests

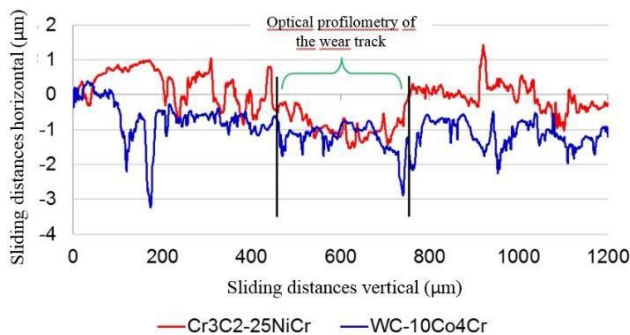


Figure 9. Topography of surface after pin-on-disc tests

4. Conclusions

Based on the results obtained it is possible to conclude that the Cr₃C₂-25NiCr and WC-10Co₄Cr coatings on the AISI H13 steel substrate are morphologically well constituted and may contribute to the reduction of surface wear. Through the microscopy analysis, the coatings were found to be homogeneous without defects, such as cracks and / or microchips, and with low porosity. Regarding the coefficient of friction, the coating of WC-10Co₄Cr is approximately 58% higher when compared to the coating of Cr₃C₂-25NiCr. However, the volume loss was more pronounced for Cr₃C₂-25NiCr coating, this is due to the lower hardness, lower adhesion and higher porosity of this coating.

For the WC-10Co₄Cr coating, which had a high hardness, there was no significant volume loss to calculate the wear rate. The adsorbed layers with Cr₃C₂-25NiCr and WC-10Co₄Cr presented satisfactory results in the analyzes carried out in this work, showing a promising future for their

application in industry components, especially regarding wear resistance.

ACKNOWLEDGEMENTS

We would like to thank the Rijeza Company from São Leopoldo for the availability to perform production tests and laboratory analysis. We acknowledge the financial support by the Brazilian agencies CAPES, CNPq (process number CNPq 311348/20157) for research grants.

REFERENCES

- [1] Souza V, Marques A, HUFF JA, Rocha A da S, Kempinski L (2016) Analysis of Forging Dies Coated with Tungsten Carbide through HVOF Processing. *J Mech Eng Autom* 6:373–378.
- [2] Lyphout C, Sato K, Houdkova S, Smazalova E, Lusvarghi L, Bolelli G, Sassatelli P (2016) Tribological Properties of Hard Metal Coatings Sprayed by High-Velocity Air Fuel Process. *J Therm Spray Technol* 25:331–345.
- [3] Lima CC, Trevisan R (2007) *Aspersão Térmica*, 2^o Edição. Artliber, São Paulo.
- [4] Fauchais PL, Heberlein JVR, Boulos MI (2014) *Thermal Spray Fundamentals*. doi: 10.1007/978-0-387-68991-3.
- [5] Murthy JKN, Rao DS, Venkataraman B (2001) Effect of grinding on the erosion behaviour of a WC-Co-Cr coating deposited by HVOF and detonation gun spray processes. *Wear* 249:592–600.
- [6] Celik E, Culha O, Uyulgan B, Ak Azem NF, Ozdemir I, Turk A (2006) Assessment of microstructural and mechanical properties of HVOF sprayed WC-based cermet coatings for a roller cylinder. *Surf Coatings Technol* 200:4320–4328.
- [7] Maiti AK, Mukhopadhyay N, Raman R (2007) Effect of adding WC powder to the feedstock of WC-Co-Cr based HVOF coating and its impact on erosion and abrasion resistance. *Surf Coatings Technol* 201:7781–7788.
- [8] Mateen A, Saha GC, Khan TI, Khalid FA (2011) Tribological behaviour of HVOF sprayed near-nanostructured and microstructured WC-17wt.%Co coatings. *Surf Coatings Technol* 206:1077–1084.
- [9] Rhys-Jones TN (1990) *Thermally Sprayed Coating Systems for Surface*. *Surf Coatings Technol* 44:402–415.
- [10] Chivavibul P, Watanabe M, Kuroda S, Komatsu M (2008) Evaluation of HVOF-sprayed WC-Co coatings for wood machining. *Surf Coatings Technol* 202:5127–5135.
- [11] Zhao L, Maurer M, Fischer F, Dicks R, Lugscheider E (2004) Influence of spray parameters on the particle in-flight properties and the properties of HVOF coating of WC-CoCr. *Wear* 257:41–46.
- [12] Yang Q, Senda T, Ohmori A (2003) Effect of carbide grain size on microstructure and sliding wear behavior of HVOF-sprayed WC-12% Co coatings. *Wear* 254:23–34.

- [13] Al-Mutairi S, Hashmi MSJ, Yilbas BS, Stokes J (2015) Microstructural characterization of HVOF/plasma thermal spray of micro/nano WC-12%Co powders. *Surf Coat Technol* 264:175–186.
- [14] Oerlikon Metco (2015) Material Product Data Sheet Tungsten Carbide – 10% Cobalt 4% Chromium Sintered and Crushed Powders for Thermal Spray. 7.
- [15] Xie M, Zhang S, Li M (2013) Comparative investigation on HVOF sprayed carbide-based coatings. *Appl Surf Sci* 273:799–805.
- [16] Metalurgica Rijeza. <http://www.rijeza.com.br>. Accessed 4 Jun 2018.
- [17] American Society for Testing and Materials (2017) ASTM E92-16. Stand Test Methods Vickers Hardness Knoop Hardness Met Mater 82:1–27.
- [18] American Society for Testing and Materials (2017) ASTM G99-17. Stand Test Method Wear Test with a Pin-on-Disk Appar 05:1–6.
- [19] Murthy JKN, Venkataraman B (2006) Abrasive wear behaviour of WC-CoCr and Cr₃C₂-20(NiCr) deposited by HVOF and detonation spray processes. *Surf Coatings Technol* 200:2642–2652.
- [20] Mudgal D, Singh S, Prakash S (2014) Evaluation of Ceria-Added Cr₃C₂-25(NiCr) Coating on Three Superalloys under Simulated Incinerator Environment. *J Therm Spray Technol* 24:496–514.
- [21] Stewart DA, Shipway PH, McCartney DG (2000) Microstructural evolution in thermally sprayed WC-Co coatings: comparison between nanocomposite and conventional starting powders. *Acta Mater* 48:1593–1604.
- [22] Berger LM (2015) Application of hardmetals as thermal spray coatings. *Int J Refract Met Hard Mater* 49:350–364.
- [23] Gaona M, Lima RS, Marple BR (2008) Influence of particle temperature and velocity on the microstructure and mechanical behaviour of high velocity oxy-fuel (HVOF)-sprayed nanostructured titania coatings. *J Mater Process Technol* 198:426–435.
- [24] Lee CW, Han JH, Yoon J, Shin MC, Kwun SI (2010) A study on powder mixing for high fracture toughness and wear resistance of WC-Co-Cr coatings sprayed by HVOF. *Surf Coatings Technol* 204:2223–2229.
- [25] Oerlikon. <https://www.oerlikon.com>. Accessed 12 Aug 2018.
- [26] Wu YS, Zeng DC, Liu ZW, Qiu WQ, Zhong XC, Yu HY, Li SZ (2011) Microstructure and sliding wear behavior of nanostructured Ni₆₀-TiB₂ composite coating sprayed by HVOF technique. *Surf Coatings Technol* 206:1102–1108.
- [27] American Society for Testing and Materials (2017) ASTM C633-13. Stand Test Method Adhes or Cohes Strength Therm Spray Coatings 03:1–7.
- [28] Asgari H, Saha G, Mohammadi M (2016) Tribological behavior of nanostructured high velocity oxy-fuel (HVOF) thermal sprayed WC-17NiCr coatings. *Ceram Int* 43: 2123–2135.
- [29] Vashishtha N, Sapate SG (2017) Abrasive wear maps for High Velocity Oxy Fuel (HVOF) sprayed WC-12Co and Cr₃C₂-25NiCr coatings. *Tribol Int* 114:290–305.
- [30] Castro RDM, Rocha S, Isaías E, Curi M, Peruch F (2018) A Comparison of Microstructural, Mechanical and Tribological Properties of WC-10Co4Cr - HVOF Coating and Hard Chrome to Use in Hydraulic Cylinders. *American Journal of Materials Science*. 8:15–26.
- [31] Heinrichs J, Jacobson S (2011) The influence from shape and size of tool surface defects on the occurrence of galling in cold forming of aluminium. *Wear* 271:2517–2524.
- [32] Menezes P.L., Nosonovsky M., Kailas S.V. LM. (2013) Friction and Wear. In: Springer (ed) *Tribol. Sci. Eng.* New York, pp 43–91.
- [33] Ludema KC (1996) Friction, Wear, Lubrication - A Textbook in Tribology. doi: 10.1017/CBO9781107415324.004S.